

© ESO 2016. All other rights are reserved. Access to this work was provided by the University of Maryland, Baltimore County (UMBC) ScholarWorks@UMBC digital repository on the Maryland Shared Open Access (MD-SOAR) platform.

Please provide feedback

Please support the ScholarWorks@UMBC repository by emailing [scholarworks-group@umbc.edu](mailto:scholarworks-group@umbc.edu) and telling us what having access to this work means to you and why it's important to you. Thank you.

LETTER TO THE EDITOR

# The MHz-peaked radio spectrum of the unusual $\gamma$ -ray source PMN J1603–4904

C. Müller<sup>1</sup>, P. R. Burd<sup>2</sup>, R. Schulz<sup>3</sup>, R. Coppejans<sup>1</sup>, H. Falcke<sup>1</sup>, H. Intema<sup>4</sup>, M. Kadler<sup>2</sup>, F. Krauß<sup>5</sup>, and R. Ojha<sup>6,7,8</sup>

<sup>1</sup> Department of Astrophysics/IMAPP, Radboud University, PO Box 9010, 6500 GL Nijmegen, The Netherlands  
e-mail: [c.mueller@astro.ru.nl](mailto:c.mueller@astro.ru.nl)

<sup>2</sup> Institut für Theoretische Physik und Astrophysik, Universität Würzburg, Am Hubland, 97074 Würzburg, Germany

<sup>3</sup> ASTRON, The Netherlands Institute for Radio Astronomy, Postbus 2, 7990 AA Dwingeloo, The Netherlands

<sup>4</sup> Leiden Observatory, Leiden University, Niels Bohrweg 2, 2333 CA Leiden, The Netherlands

<sup>5</sup> GRAPPA & Anton Pannekoek Institute for Astronomy, University of Amsterdam, Science Park 904, 1098 XH Amsterdam, The Netherlands

<sup>6</sup> NASA, Goddard Space Flight Center, Astrophysics Science Division, Code 661, Greenbelt, MD 20771, USA

<sup>7</sup> CRESST/University of Maryland Baltimore County, Baltimore, MD 21250, USA

<sup>8</sup> Catholic University of America, Washington, DC 20064, USA

Received 18 August 2016 / Accepted 4 September 2016

## ABSTRACT

**Context.** The majority of bright extragalactic  $\gamma$ -ray sources are blazars. Only a few radio galaxies have been detected by *Fermi*/LAT. Recently, the GHz-peaked spectrum source PKS 1718–649 was confirmed to be  $\gamma$ -ray bright, providing further evidence for the existence of a population of  $\gamma$ -ray loud, compact radio galaxies. A spectral turnover in the radio spectrum in the MHz to GHz range is a characteristic feature of these objects, which are thought to be young due to their small linear sizes. The multiwavelength properties of the  $\gamma$ -ray source PMN J1603–4904 suggest that it is a member of this source class.

**Aims.** The known radio spectrum of PMN J1603–4904 can be described by a power law above 1 GHz. Using observations from the Giant Metrewave Radio Telescope (GMRT) at 150, 325, and 610 MHz, we investigate the behavior of the spectrum at lower frequencies to search for a low-frequency turnover.

**Methods.** Data from the TIFR GMRT Sky Survey (TGSS ADR) catalog and archival GMRT observations were used to construct the first MHz to GHz spectrum of PMN J1603–4904.

**Results.** We detect a low-frequency turnover of the spectrum and measure the peak position at about 490 MHz (rest-frame), which, using the known relation of peak frequency and linear size, translates into a maximum linear source size of  $\sim 1.4$  kpc.

**Conclusions.** The detection of the MHz peak indicates that PMN J1603–4904 is part of this population of radio galaxies with turnover frequencies in the MHz to GHz regime. Therefore it can be considered the second confirmed object of this kind detected in  $\gamma$ -rays. Establishing this  $\gamma$ -ray source class will help to investigate the  $\gamma$ -ray production sites and to test broadband emission models.

**Key words.** galaxies: active – galaxies: jets – galaxies: individual: PMN J1603–4904

## 1. Introduction

Most sources detected at  $\gamma$ -ray energies by the *Fermi* Large Area Telescope (LAT) are active galactic nuclei (AGN), in particular blazars, which are extragalactic jets observed at small angles to the line of sight (Acero et al. 2015). Only a few, nearby non-blazar sources are detected (see also, e.g., Abdo et al. 2010b; Acero et al. 2015). In contrast to blazars, jets in radio galaxies or misaligned sources are seen at larger inclination angles, hence, they are less or not at all relativistically beamed. A typical broadband spectrum can be explained by inverse Compton or hadronic processes in the jet (see, e.g., Massaro et al. 2016, and references therein). The location and mechanism of the high-energy emission are still subject to much debate. Possible origins include core, parsec-scale jets, and the kiloparsec-scale lobes. In nearby sources (Centaurus A and Fornax A, Abdo et al. 2010a; Ackermann et al. 2016b) the  $\gamma$ -ray emission from the lobes can be directly imaged with the *Fermi*/LAT.

The smaller versions of evolved radio galaxies are of a few kpc or less in size (e.g., Readhead et al. 1996a,b; O’Dea 1998; Kunert-Bajraszewska et al. 2010). Since their morphologies are reminiscent of the evolved double sources, they

are called compact symmetric objects’ ( $\lesssim 1$  kpc, CSOs) or medium-sized symmetric objects’ ( $\lesssim 1\text{--}15$  kpc, MSOs). Kinematic measurements of their compact lobes suggest that these sources are younger than full-sized radio galaxies (e.g., Owsianik & Conway 1998; An et al. 2012). An alternative explanation of the smaller extensions is the scenario of frustrated jets, i.e., the source is confined owing to the interaction with a dense, surrounding medium (Bicknell et al. 1997; Carvalho 1998). Thus, these sources play an important role in the study of AGN evolution and the interaction of AGN jets with the ambient medium.

Typically, CSOs show a turnover or cutoff in their radio flux-density spectrum around 1 GHz, where the spectrum changes from flat or steep at higher frequencies to an inverted spectrum. The peak of MSOs is typically lower, in the upper megahertz range. The convex spectral shape of their radio spectrum is one of the defining properties of these small radio sources. Based on the peak frequency  $\nu_{\text{peak}}$ , one refers to MHz-peaked spectrum (MPS) or compact steep spectrum (CSS) sources for  $\nu_{\text{peak}} < 1$  GHz and GHz-peaked sources (GPS) for  $\nu_{\text{peak}} > 1$  GHz (O’Dea 1998).

The reason for this turnover could be either due to synchrotron self-absorption (SSA; e.g., Snellen et al. 2000) by relativistic electrons from the emitting source, or free-free absorption due to an external dense medium (FFA; e.g., Bicknell et al. 1997). Well-sampled radio spectra are necessary to identify the underlying absorption mechanism (e.g., Callingham et al. 2015).

Several studies found that the linear size  $LS$  of the radio morphology anticorrelates with the rest-frame peak frequency of the radio spectrum (Fanti et al. 1995; O’Dea & Baum 1997; O’Dea 1998),

$$\log \nu_{\text{peak}} \approx -0.21(\pm 0.05) - 0.65(\pm 0.05) \log LS, \quad (1)$$

with  $LS$  in kpc and  $\nu_{\text{peak}}$  in GHz. This relation indicates that the mechanism causing the spectral turnover is related to the source size and is explained well in the SSA scenario. Therefore, a typical GPS radio galaxy has an extent of less than 1 kpc. A typical MPS or CSS is up to 20 kpc in size according to this relation.

Evolved radio galaxies have been established as  $\gamma$ -ray loud objects (e.g., Abdo et al. 2010b). Theoretical broadband emission models also (Kino et al. 2009; Kino & Asano 2011; Kino et al. 2013; Stawarz et al. 2008; Ostorero et al. 2010) predict  $\gamma$ -ray emission from compact, likely young, radio galaxies. Because of the interaction of the evolving radio source and the interstellar medium, high-energy emission can be produced through the non-thermal inverse Compton process or thermal bremsstrahlung. The interaction of particles in the lobes with the ambient medium is expected to dominate the emission, while the contribution of the jet is smaller because of Doppler de-boosting (Stawarz et al. 2008). Kino et al. (2009) predict thermal bremsstrahlung  $\gamma$ -ray emission in the initial phase of expansion at a detectable level for *Fermi*/LAT observations of nearby young radio galaxies.

Two CSS sources, 3FGL J1330.5+3023 (3C 286) and 3FGL J0824.9+3916 (4C +39.23B), were reported in the latest *Fermi*/LAT AGN catalog (3LAC, Ackermann et al. 2015). However, GPS sources are still not confirmed as a  $\gamma$ -ray bright source class. Only recently, Migliori et al. (2016) reported of the first detection of an established CSO/GPS, PKS 1718–649. This result follows the discussions of a few  $\gamma$ -ray CSO-candidates detected by *Fermi*/LAT (see also D’Ammando et al. 2016, for a summary): 4C+55.1 (McConville et al. 2011), PKS 1413+135 (Gugliucci et al. 2005), 2234+282 (An et al. 2016), and PMN J1603–4904 (Müller et al. 2014).

An extensive multiwavelength study of PMN J1603–4904 (Müller et al. 2014, 2015), conducted within the framework of the TANAMI program (Ojha et al. 2010; Kadler et al. 2015), suggested it was not a blazar. Very Long Baseline Interferometry (VLBI) observations indicate a CSO-like morphology. The kinematic study on timescales of  $\sim 15$  months shows no significant motion of the eastern and western component. Lower resolution radio observations with the ATCA ( $>1$  GHz) indicate extended, unresolved emission at sub-arcsecond scales. X-ray observations with *XMM-Newton* and *Suzaku* measure an emission line in the X-ray spectrum on top of an absorbed power-law emission. Together with the optical-spectroscopic redshift of  $z = 0.23$  from X-shooter observations (Goldoni et al. 2016) this X-ray feature could be interpreted as emission from a highly ionized plasma, but the lack of a neutral iron line is puzzling. The *Fermi*/LAT counterpart 3FGL 1603.9–4903 (with 95%-confidence semimajor axis of  $\sim 0.8$  arcmin)<sup>1</sup> shows a hard  $\gamma$ -ray spectrum but

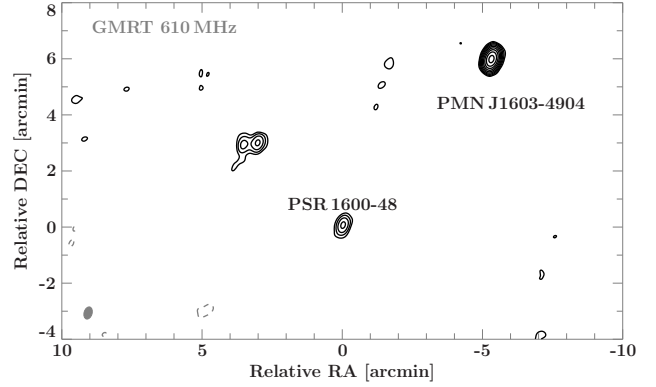


**Fig. 1.** Radio map at 610 MHz observed with the GMRT. The  $x$ - and  $y$ -axis give relative angular distances to the pulsar PSR 1600–48 in right ascension and declination, respectively. An unclassified double source and PMN J1603–4904, the brightest source in that region, are clearly detected. The contours indicate the flux density level, scaled logarithmically with the lowest level set to the  $3\sigma$  noise level. The restoring beam is shown as a gray ellipse in the lower left corner.

with a spectral break above 50 GeV and only mild variability (Ackermann et al. 2013, 2016a; Acero et al. 2015). These broadband properties led to the conclusion that PMN J1603–4904 is either a very peculiar blazar or a compact, possibly young, radio galaxy. Opposite motion of the radio lobes and a turnover in the radio spectrum would hence be expected and would further confirm the CSO nature.

Here we present a detailed analysis of the radio spectrum of PMN J1603–4904, extending the existing information down to 150 MHz.

## 2. Observations and data reduction

The analysis of the radio spectrum presented in Müller et al. (2014) shows that the PMN J1603–4904 spectrum above  $\geq 1$  GHz follows a power law with a spectral index (defined as  $S_\nu \sim \nu^{+\alpha}$ ) of  $\alpha \sim -0.35$  (see Sect. 3). The lowest ATCA frequency is  $\sim 1$  GHz, hence, besides one archival spectral point at 843 GHz (Murphy et al. 2007), no spectral information in the MHz regime was available.

With the recent release of the catalog from the TIFR GMRT Sky Survey (TGSS ADR; Intema et al. 2016) from the Giant Metrewave Radio Telescope (GMRT; Swarup 1991), the first low-frequency information on PMN J1603–4904 became available. The TGSS catalog contains 150 MHz all-sky survey data obtained between 2010 and 2012, covering the sky north of  $-53^\circ$  declination with an approximate resolution of  $\sim 25'' \times 25''/\cos(\text{Dec} - 19^\circ)$  for  $\text{Dec} < 19^\circ$ , otherwise  $25''$  circular. The unresolved catalog source J160350.7–490405 can be associated with PMN J1603–4904. It has a flux density of  $702.3 \pm 71.6$  mJy and is modeled with a single Gaussian component of  $\sim 25.3'' \times 68.5''$ .

Following this result, we analyzed archival GMRT data of PMN J1603–4904 at 325 GHz (project code: 25\_038, observation date: 2014-01-31) and 610 GHz (25\_038, observation date: 2014-03-23). These observations were pointed at the pulsar PSR 1600–48. The large field of view of the GMRT observations ( $\sim 43$  arcmin at 610 MHz) also allowed us to detect PMN J1603–4904 which has a distance from the pulsar of about  $\sim 8$  arcmin. The GMRT data were calibrated using the Astronomical Imaging Processing System (AIPS; Greisen 2003). Since GMRT data are strongly influenced by radio frequency interference (RFI),

<sup>1</sup> A false association of the  $\gamma$ -ray source with PMN J1603–4904 is still possible, however, as pointed out in Müller et al. (2015) a more exotic explanation for the  $\gamma$ -ray emission origin would be required.

**Table 1.** MHz flux densities of PMN J1603–4904.

$\nu_{\text{obs}}$ [MHz]	$S_{\nu, \text{measured}}$ [Jy]	$S_{\nu, \text{corrected}}$ [Jy]	Reference
150	–	$0.702 \pm 0.072$	TGSS
300	$0.61 \pm 0.07$	$2.18 \pm 0.23$	this work
600	$1.21 \pm 0.10$	$1.91 \pm 0.25$	this work
843	$1.54 \pm 0.5$	–	MGPS

we used one channel that is not corrupted to perform the amplitude calibration. Using the flux calibrator 3C 286 we calibrated the amplitudes of PMN J1603–4904 for the given channel and applied a bandpass calibration afterward (using AIPS task BPASS). Note that PMN J1603–4904 is not resolved, therefore we did not calibrate the phases. With the AIPS task FLGIT we flagged RFI noise. Afterward we channel averaged and exported the data to DIFMAP (Shepherd 1997), where we used an iterative self-calibration procedure to image the field. We used Gaussian model fits to obtain the flux densities of the individual sources. We are only interested in the central part of the map (inner  $\sim 10$  arcmin) and not in the detailed structure of the sources, hence, bandwidth smearing and non-coplanar baseline effects (w-projection) are not an issue. GMRT data are prone to flux scale errors due to sky temperature differences between the flux calibrator and target field (e.g., Marcote et al. 2015). Following Intema et al. (2016), the radio images at 325 and 610 MHz were corrected for this effect by a scaling factor depending on frequency and sky position. For PMN J1603–4904 these correction factors are  $3.56 \pm 0.2$  for 325 MHz and  $1.58 \pm 0.2$  for 610 MHz. In order to account for systematic errors we add a 10% uncertainty (Chandra et al. 2004). A summary of the available MHz data of PMN J1603–4904 can be found in Table 1.

Figure 1 shows the resulting 610 MHz image of the field, clearly showing the detection of the pulsar (phase center), a double source to the northeast (TGSS-IDs: J160444.6–490703 and J160444.7–490703) and PMN J1603–4904, which is unresolved at both frequencies.

### 3. The MHz to GHz spectrum of PMN J1603–4904

The previous analysis of the GHz radio data in Müller et al. (2014) revealed no variability below  $\sim 20$  GHz since 2000, hence, we expect that PMN J1603–4904 exhibits no major flux change at sub-GHz frequencies over this time period. With this assumption we construct a non-simultaneous MHz to GHz spectrum of PMN J1603–4904. Figure 2 shows the resulting radio spectrum including all available archival data points, i.e., the data presented in Müller et al. (2014), measurements from the ALMA calibrator database<sup>2</sup>, and the new MHz measurements from GMRT.

The spectrum clearly shows a turnover at  $\sim 400$  MHz (observed frame). Such a turnover in the radio regime of an AGN spectrum can be either due to SSA or FFA. We test both models, using the SSA model

$$S_{\nu, \text{SSA}} = a_{\text{SSA}} \nu^{+2.5} \left[ 1 - \exp(-\tau_{\text{SSA}} \nu^{\alpha-2.5}) \right] \quad (2)$$

and the FFA model

$$S_{\nu, \text{FFA}} = a_{\text{FFA}} \nu^{\alpha} \exp(-\tau_{\text{FFA}} \nu^{-2.1}) \quad (3)$$

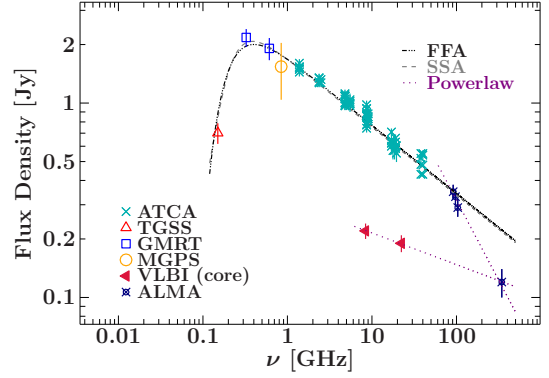


**Fig. 2.** Radio spectrum of PMN J1603–4904 including archival data points from the ATCA, VLBI (Müller et al. 2014), MGPS (Murphy et al. 2007), the ALMA calibrator survey, TGSS (Intema et al. 2016), and GMRT (this work). The low-resolution data (i.e., except VLBI core fluxes) can be well described by a FFA (black) or SSA (gray) spectrum with a spectral turnover at  $\sim 400$  MHz (observed frame). The highest measurement at 343.5 GHz by ALMA could either be due to a spectral break around 100 GHz or emission of the inner jet indicated by the power-law spectrum defined by the VLBI core (see Sect. 3).

**Table 2.** Spectral fit parameters.

Model	$a$	$\tau$	$\nu_{\text{turnover}}^a$ [GHz]	$\chi^2_{\text{red}}$
FFA	$1.7 \pm 0.2$	$0.02 \pm 0.01$	$0.40 \pm 0.04$	4.4
SSA	$98 \pm 24$	$0.02 \pm 0.01$	$0.39 \pm 0.03$	4.5

**Notes.** <sup>(a)</sup> Observed-frame peak or turnover frequency of the spectrum.

with the spectral index  $\alpha$  and the SSA or FFA absorption coefficient  $\tau_{\text{SSA/FFA}}$ , respectively (following the definition by Kameno et al. 2003). We use  $\alpha = -0.35$  from a fit to the ATCA and ALMA data above  $>1$  GHz. We fit all data, which are all from unresolved images, except the core fluxes from VLBI.

Both models can describe the data equally well (see Fig. 2 and Table 2). The  $\chi^2_{\text{red}}$  values are comparable to results by Callingham et al. (2015) who discussed FFA and SSA models for the GPS source PKS B0008–421. The authors stress that more densely sampled data below the turnover would be required to distinguish between the absorption mechanisms. The spectral coverage allows us to constrain the spectral turnover of PMN J1603–4904 at  $\sim 400$  MHz (observed frame), but not to check more sophisticated models. Using the anticorrelation between rest-frame peak frequency (i.e.,  $\sim 490$  MHz at  $z = 0.23$ ) and size (see Eq. (1)) from O’Dea & Baum (1997) we can estimate the maximum size of PMN J1603–4904 to be  $\sim 1.4$  kpc. This is close to the canonical limit of 1 kpc for CSOs (O’Dea 1998) and well within the limits for MSOs.

At  $\geq 100$  GHz, the ALMA measurement at 343.5 GHz (Band 7) could indicate a break in the synchrotron spectrum. A power-law fit to the ALMA data only yields  $\alpha_{\text{ALMA}} \sim -0.8$ . Such a spectral break could be explained by radiation losses. The VLBI analysis shows that about 20% of the extended emission detected by the ATCA is resolved out (Müller et al. 2014). A power-law fit to the VLBI core flux densities at 8 and 22 GHz and the ALMA Band 7 measurement yields a spectral index of  $\alpha_{\text{core}} \sim -0.16$ . The Band 7 measurement basically presents the extrapolation of the core spectrum. Taking the known source geometry into account, it is more plausible that the jet or core is dominating the overall emission at these high frequencies, while at lower energies the emission of the large-scale structure, beyond VLBI scales, can be detected.

<sup>2</sup> <https://almascience.eso.org/alma-data/calibrator-catalogue>

## 4. Conclusions

We have presented the first MHz to GHz spectrum for the  $\gamma$ -ray loud extragalactic jet source PMN J1603–4904. The radio spectrum clearly shows a rest-frame spectral turnover at  $\sim 490$  MHz. Using the established anticorrelation of peak frequency and linear size, we determine the linear size of PMN J1603–4904 to be  $\sim 1.4$  kpc. With VLBI, only the inner  $\sim 40$  pc of the small radio source are detected (Müller et al. 2014). The spectral index of the optically thin emission is comparably flat for GPS or CSS sources (O’Dea 1998; Fanti et al. 2001), and is likely due to the bright compact emission. The spectral shape can be explained by the superposition of different components. Both, the SSA and FFA models can describe the overall spectrum. The turnover can hence be attributed either to self-absorption or to external absorption by a dense medium.

The sparse spectral coverage below 1 GHz does not allow the testing of more complex models or distinguishing between SSA and FFA. More sensitive observations with southern telescopes like the upgraded GMRT (Rao Bandari et al. 2013) or the Murchinson Widefield Array (MWA; Tingay et al. 2013), covering a wider frequency range in the MHz regime would be required. Higher resolution observations with sufficient sensitivity could allow us to image the extended emission. Currently, only ALMA is capable of addressing these scales at this low declination.

Because of its multiwavelength properties, PMN J1603–4904 has been discussed as a possible  $\gamma$ -ray loud young radio galaxy. With the observations reported here, this classification is supported by the detection of an MPS-like radio spectrum. PMN J1603–4904 adds to the class of so far very rare extragalactic jets that show a spectral turnover in the MHz to GHz range, and are detected at  $\gamma$ -rays. As it is the second confirmed object of this type, following PKS 1718–649 (Migliori et al. 2016), there are some noteworthy differences. First, PKS 1718–649 is a nearby galaxy ( $z = 0.014$ ) in contrast to PMN J1603–4904 at  $z = 0.23$ . Furthermore, PMN J1603–4904 has a hard GeV spectrum with a photon index  $\Gamma \sim 2$  (Abdo et al. 2010; Nolan et al. 2012; Acero et al. 2015), while for PKS 1718–649 a  $\Gamma \sim 2.9$  was found (Migliori et al. 2016), that is more comparable with the spectrum of the Cen A lobes (Abdo et al. 2010a). Hence, as also discussed by Migliori et al. (2016), this could indicate significant differences in the intrinsic physical mechanism producing  $\gamma$ -rays. This is also suggested by the VLBI structure of both sources: while PKS 1718–649 has an irregular lobe-dominated morphology (Tingay & de Kool 2003; Ojha et al. 2010), PMN J1603–4904 is a more symmetric, core dominated source.

Future *Fermi*/LAT observations using the Pass8 analysis (Atwood et al. 2013) will have the required sensitivity to detect further GPS and CSS sources at  $\gamma$ -rays. By establishing this source class and its defining properties one will be able to test theoretical emission models (e.g., Kino et al. 2007, 2009; Stawarz et al. 2008). For PMN J1603–4904, modeling of the broadband SED will help us to understand the high-energy emission mechanism. The high Compton dominance (see Fig. 7 in Müller et al. 2014) and the flat  $\gamma$ -ray spectrum challenges current models.

**Acknowledgements.** We thank the anonymous referee for the prompt review and T. Beuchert for helpful comments that improved the manuscript. We thank the staff of the GMRT that made these observations possible. GMRT is run by the National Centre for Radio Astrophysics of the Tata Institute of Fundamental Research. This paper makes use of ALMA calibrator database: <https://almascience.eso.org/alma-data/calibrator-catalogue>. ALMA is a partnership of ESO (representing its member states), NSF (USA) and NINS

(Japan), together with NRC (Canada), NSC and ASIAA (Taiwan), and KASI (Republic of Korea), in cooperation with the Republic of Chile. The Joint ALMA Observatory is operated by ESO, AUI/NRAO and NAOJ. C.M. and H.F. acknowledge support from the ERC Synergy Grant “BlackHoleCam – Imaging the Event Horizon of Black Holes” (Grant 610058). F.K. acknowledges funding from the European Union’s Horizon 2020 research and innovation program under grant agreement No. 653477. R.S. acknowledges support from the ERC under the European Union’s Seventh Framework Programme (FP/2007-2013)/ERC Advanced Grant RADIOLIFE-320745. This research was funded in part by NASA through Fermi Guest Investigator grant NNH13ZDA001N-FERMI.

## References

- Abdo, A. A., Ackermann, M., Ajello, M., et al. 2010, *ApJS*, **188**, 405
- Abdo, A. A., Ackermann, M., Ajello, M., et al. 2010a, *Science*, **328**, 725
- Abdo, A. A., Ackermann, M., Ajello, M., et al. 2010b, *ApJ*, **720**, 912
- Acero, F., Ackermann, M., Ajello, M., et al. 2015, *ApJS*, **218**, 23
- Ackermann, M., Ajello, M., Allafort, A., et al. 2013, *ApJS*, **209**, 34
- Ackermann, M., Ajello, M., Atwood, W. B., et al. 2015, *ApJ*, **810**, 14
- Ackermann, M., Ajello, M., Atwood, W. B., et al. 2016a, *ApJS*, **222**, 5
- Ackermann, M., Ajello, M., Baldini, L., et al. 2016b, *ApJ*, **826**, 1
- An, T., Wu, F., Yang, J., et al. 2012, *ApJS*, **198**, 5
- An, T., Cui, Y.-Z., Gabányi, K. É., et al. 2016, *Astron. Nachr.*, **337**, 65
- Atwood, W., Albert, A., Baldini, L., et al. 2013, in 2012 Fermi Symposium proceedings, eConf Proceedings C121028 [[arXiv:1303.3514](https://arxiv.org/abs/1303.3514)]
- Bicknell, G. V., Dopita, M. A., & O’Dea, C. P. O. 1997, *ApJ*, **485**, 112
- Callingham, J. R., Gaensler, B. M., Ekers, R. D., et al. 2015, *ApJ*, **809**, 168
- Carvalho, J. C. 1998, *A&A*, **329**, 845
- Chandra, P., Ray, A., & Bhatnagar, S. 2004, *ApJ*, **612**, 974
- D’Ammando, F., Orienti, M., Giroletti, M., & Fermi Large Area Telescope Collaboration 2016, *Astron. Nachr.*, **337**, 59
- Fanti, C., Fanti, R., Dallacasa, D., et al. 1995, *A&A*, **302**, 317
- Fanti, C., Pozzi, F., Dallacasa, D., et al. 2001, *A&A*, **369**, 380
- Goldoni, P., Pita, S., Boisson, C., et al. 2016, *A&A*, **586**, L2
- Greisen, E. W. 2003, *Information Handling in Astronomy – Historical Vistas*, **285**, 109
- Gugliucci, N. E., Taylor, G. B., Peck, A. B., & Giroletti, M. 2005, *ApJ*, **622**, 136
- Intema, H. T., Jagannathan, P., Mooley, K. P., & Frail, D. A. 2016, *A&A*, submitted [[arXiv:1603.04368](https://arxiv.org/abs/1603.04368)]
- Kadler, M., Ojha, R., & TANAMI Collaboration 2015, *Astron. Nachr.*, **336**, 499
- Kamenno, S., Inoue, M., Wajima, K., Sawada-Satoh, S., & Shen, Z.-Q. 2003, *PASA*, **20**, 213
- Kino, M., & Asano, K. 2011, *MNRAS*, **412**, L20
- Kino, M., Ito, H., Kawakatu, N., & Nagai, H. 2009, *MNRAS*, **395**, L43
- Kino, M., Kawakatu, N., & Ito, H. 2007, *MNRAS*, **376**, 1630
- Kino, M., Ito, H., Kawakatu, N., & Orienti, M. 2013, *ApJ*, **764**, 134
- Kunert-Bajraszewska, M., Gawroński, M. P., Labiano, A., & Siemiginowska, A. 2010, *MNRAS*, **408**, 2261
- Marcote, B., Ribó, M., Paredes, J. M., & Ishwara-Chandra, C. H. 2015, *MNRAS*, **451**, 59
- Massaro, F., Thompson, D. J., & Ferrara, E. C. 2016, *A&ARv*, **24**, 2
- McConville, W., Ostorero, L., Moderski, R., et al. 2011, *ApJ*, **738**, 148
- Migliori, G., Siemiginowska, A., Sobolewska, M., et al. 2016, *ApJ*, **821**, L31
- Müller, C., Kadler, M., Ojha, R., et al. 2014, *A&A*, **562**, A4
- Müller, C., Krauß, F., Dauser, T., et al. 2015, *A&A*, **574**, A117
- Murphy, T., Mauch, T., Green, A., et al. 2007, *MNRAS*, **382**, 382
- Nolan, P. L., Abdo, A. A., Ackermann, M., et al. 2012, *ApJS*, **199**, 31
- O’Dea, C. P. 1998, *PASP*, **110**, 493
- O’Dea, C. P., & Baum, S. A. 1997, *AJ*, **113**, 148
- Ojha, R., Kadler, M., Böck, M., et al. 2010, *A&A*, **519**, A45
- Ostorero, L., Moderski, R., Stawarz, L., et al. 2010, *ApJ*, **715**, 1071
- Owsianik, I., & Conway, J. E. 1998, *A&A*, **337**, 69
- Rao Bandari, H., Sankarasubramanian, G., & Praveen Kumar, A. 2013, *Mat. Sci. Eng. Conf. Ser.*, **44**, 012023
- Readhead, A. C. S., Taylor, G. B., Pearson, T. J., & Wilkinson, P. N. 1996a, *ApJ*, **460**, 634
- Readhead, A. C. S., Taylor, G. B., Xu, W., et al. 1996b, *ApJ*, **460**, 612
- Shepherd, M. C. 1997, in *Astronomical Data Analysis Software and Systems VI*, ed. G. Hunt & H. Payne, *ASP Conf. Proc.*, **125**, 77
- Snellen, I. A. G., Schilizzi, R. T., Miley, G. K., et al. 2000, *MNRAS*, **319**, 445
- Stawarz, L., Ostorero, L., Begelman, M. C., et al. 2008, *ApJ*, **680**, 911
- Swarup, G. 1991, in *Theory, Techniques, and Applications*, eds. T. J. Cornwell & R. A. Perley (IAU Colloq. 131: Radio Interferometry), *ASP Conf. Ser.*, **19**, 376
- Tingay, S. J., & de Kool, M. 2003, *AJ*, **126**, 723
- Tingay, S. J., Goeke, R., Bowman, J. D., et al. 2013, *PASA*, **30**, e007